Supplementary Information File

Analysis of gating transitions among the three major open states of the OpdK channel[†]

Belete R. Cheneke,[‡] Bert van den Berg,[§] and Liviu Movileanu[*,‡,&,#]

[‡]*Department of Physics, Syracuse University, 201 Physics Building, Syracuse, New York 13244-1130, USA*

[§]*Program in Molecular Medicine, University of Massachusetts Medical School, Worcester, Massachusetts 01605, USA*

[&]*Structural Biology, Biochemistry, and Biophysics Program, Syracuse University, 111 College Place, Syracuse, New York 13244-4100, USA*

[#]*Syracuse Biomaterials Institute, Syracuse University, 121 Link Hall, Syracuse, New York 13244, USA*

Running title: The three-state kinetics of a protein

Key words: • Spontaneous gating; • Single-molecule biophysics; • Single-channel electrical recordings; • The OpdK protein; • The kinetic rate theory; • The OprD family.

[†]This paper is funded in part by grants from the US National Science Foundation (DMR-0706517 and DMR-1006332, L.M.) and the National Institutes of Health (R01 GM088403, L.M. and R01 GM085785, B.v.d.B).

[*]**Corresponding author:** Department of Physics, Syracuse University, 201 Physics Building, Syracuse, New York 13244-1130, USA; Phone: 315-443-8078; Fax: 315-443-9103;

E-mail: lmovilea@physics.syr.edu

Table S1. Physical features of the extracellular loops of the WT-OpdK protein (*1*).

Loops	Residues (position in sequence)	Total residues	Charges	Range of the B-factor*	Average B-factor*
L1	RDHDAGKSL (25-33)	9	-2/+2	54.1 - 65.0	60.6 ± 5.7
L2	LNSGRGTSNSELLPLHDDGR AAD (68-90)	23	-4/+2	44.2 - 66.4	51.3 ± 6.4
L3	GEMLPDIPLLRYDDGRLLPQ (111-130)	20	-4/+2	19.6 - 28.5	23.4 ± 2.7
L4	LRNSADMQDLSAWSAPTQK SDG (157-178)	22	-3/+2	24.3 - 35.8	30.0 ± 2.8
L5	ED (203-204)	2	-2/0	25.5 - 27.2	26.4 ± 1.2
L6	DGAARAGEI (236-244)	9	-2/+1	26.7 - 36.9	30.7 ± 3.7
L7	GDSGWQSVYGSSGRSMGN DMFNGNFTNADE (271-300)	30	-4/+1	17.8 - 57.3	24.8 ± 7.2
L8	NATTKAGSGGK (330-340)	11	0/+2	26.6 - 47.5	36.2 ± 7.3
L9	SFNSD (372-376)	5	-1/0	28.8 - 34.9	32.1 ± 2.3

*The last two columns indicate the range of the temperature B-factor based upon the C_α atoms and the average B-factor of the fluctuating loop.

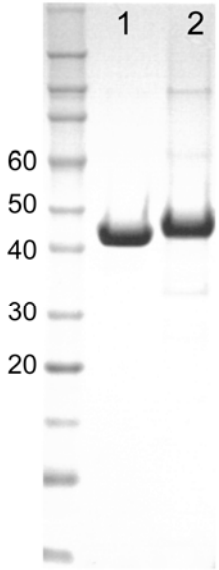

<u>Figure S1:</u> Purification of *P. aeruginosa* OpdK used for single-channel electrical recordings. SDS-PAGE gel showing the final sample of OpdK after cleavage of the N-terminal hepta-histidine tag by TEV protease (Lane 1). The protein before cleavage is shown in Lane 2. The molecular weights of marker proteins are shown on the left side (Novex Sharp Standard, Invitrogen). An amount of 3 μg OpdK protein was loaded on each lane.

Standard histograms of fitted current amplitudes

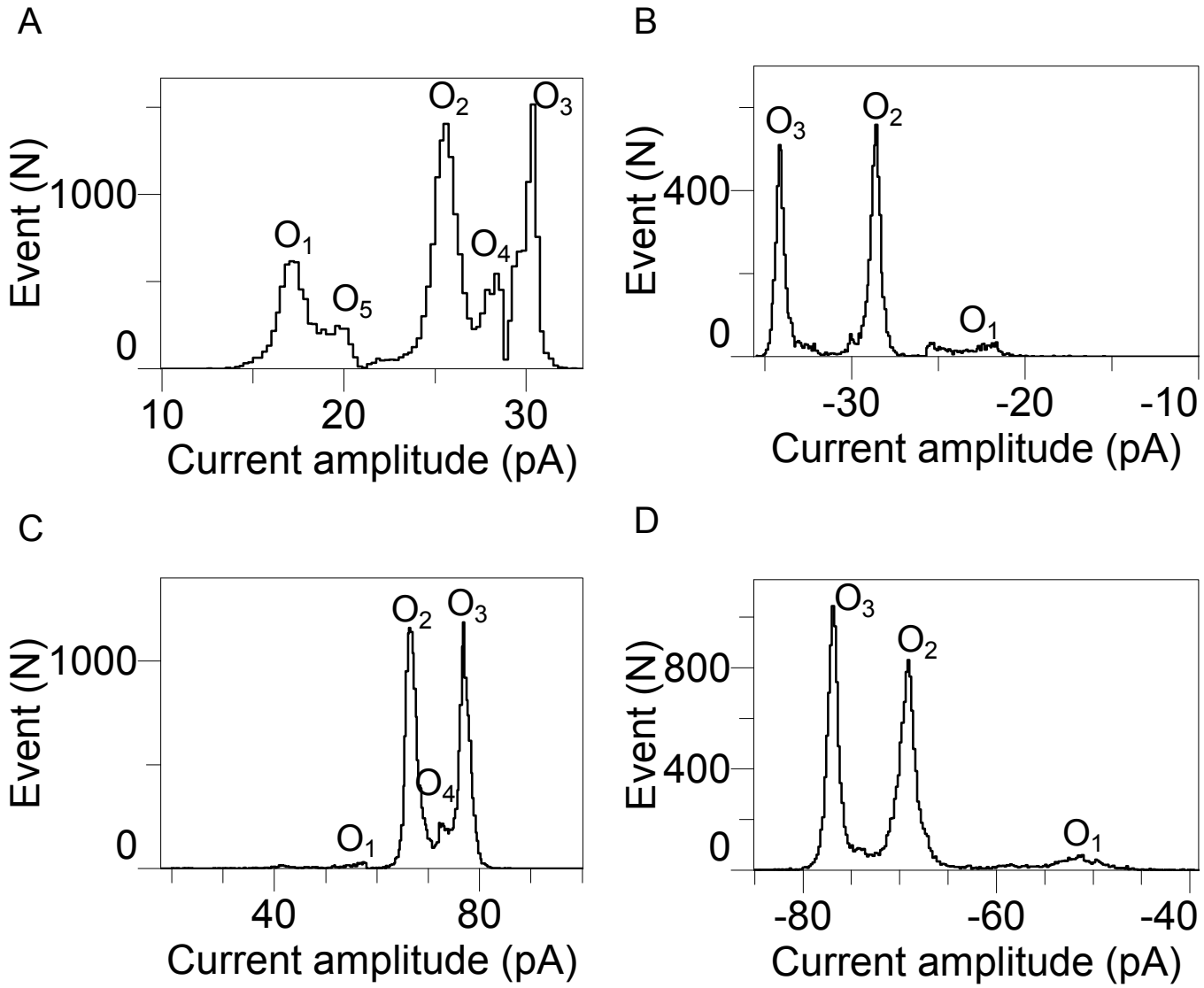

Figure S2: Typical standard histograms of fitted current amplitudes, which were resulted from event-list protocol in ClampFit software (Axon). The vertical axis represents the number of events in the respective peak. **(A)** The transmembrane potential was +80 mV. The data were acquired in 1 M KCl. The conditions were the same as in **Fig. 2**, the main text. The panel shows contaminations of the open O_4 and O_5 sub-states; **(B)** The transmembrane potential was -80 mV. The data were acquired in 1 M KCl. The conditions were the same as in **Fig. 3**, the main text; **(C)** The transmembrane potential was +80 mV. The data were acquired in 4 M KCl. The conditions were the same as in **Fig. 4**, the main text; **(D)** The transmembrane potential was -80 mV. The data were acquired in 4 M KCl. The conditions were the same as in **Fig. 5**, the main text.

Single-channel electrical trace of the WT-OpdK protein at a lower temperature

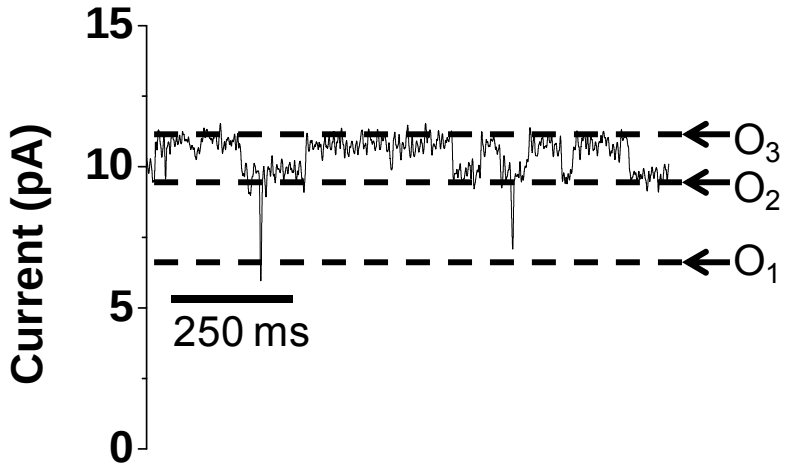

Figure S3: The wild-type OpdK protein pore exhibits a three-state discrete channel kinetics under a broad range of conditions. The figure show a single-channel electrical trace acquired in 2 M KCl, 10 mM potassium phosphate, pH 7.4 at 4°C. The applied transmembrane potential was +40 mV. For the sake of clarity, the trace was low-pass Bessel filtered at 200 Hz.

Temperature controller for single-channel electrical recordings with planar lipid bilayers. The temperature-control experiments were carried out by using a Dagan HCC-100A controller (Dagan Corporation, Minneapolis, MN), which was adapted to planar bilayer recordings (*2*;*3*). The HCC-100A heats and cools an aluminum thermal stage through Peltier elements. The temperature was computer-controlled through an external command connection via the Digidata 1322A (Axon). Temperature was simultaneously monitored in the aluminum stage and in the bilayer chamber with thermocouple probes.

Table S2. Properties of the loop-deletion OpdK mutants.

Loop	Deleted Residues	Charges	Number of residues	Salt Bridges
L3	124-129 (DGRLLP)	1/-1	6	Asp124-Arg16 Arg126-Glu78
L4	166-175 (LSAWSAPTQK)	1/0	10	None
L7	281-287 (SSGRSMG)	1/0	7	Arg284-Asp116

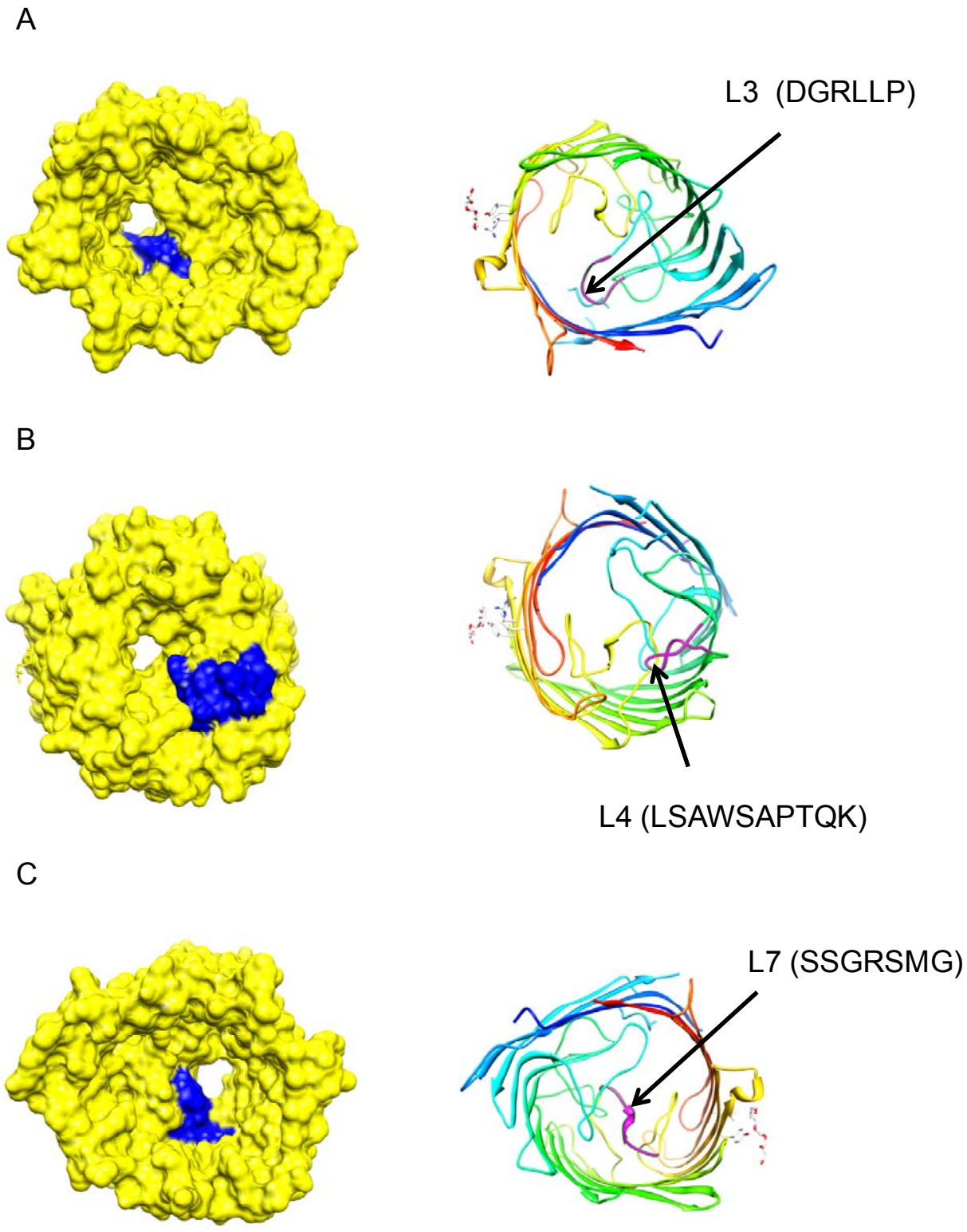

Figure S4: Locations of the loop deletions examined in this work.

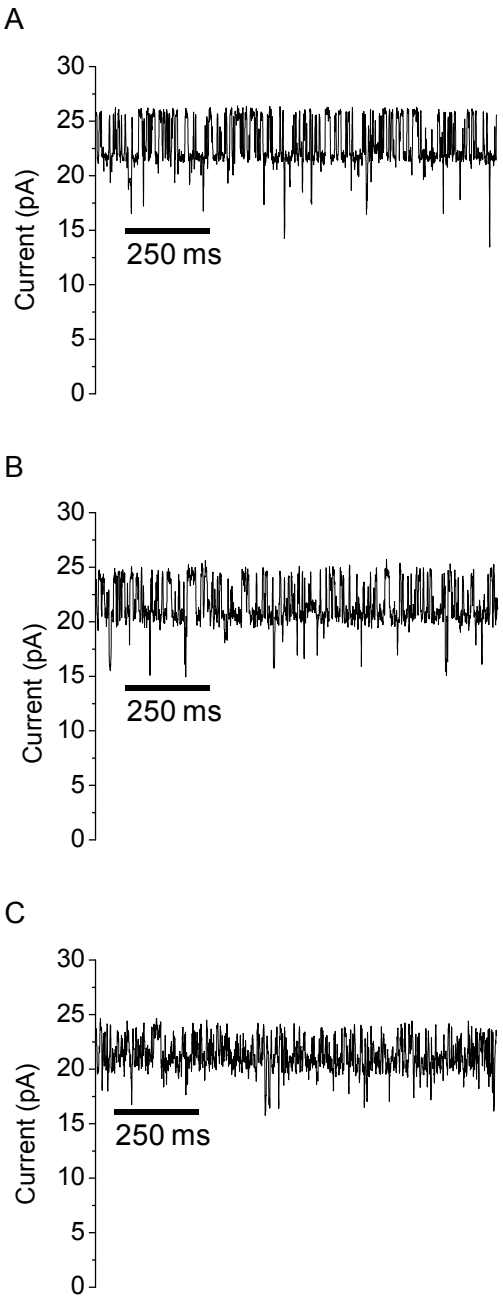

Figure S5: Single-channel electrical recordings with loop-deletion OpdK mutants. **(A)** OpdK; **(B)** OpdK ΔL3; **(C)** OpdK ΔL4. The single-channel electrical recordings were acquired in 2 M KCl, 10 mM potassium phosphate, pH 8.0. The applied transmembrane potential was +40 mV. For the sake of clarity, the electrical traces were low-pass Bessel filtered at 200 Hz.

A three-state kinetic model for the current fluctuations of the wild-type OpdK protein.

Using standard formalisms of chemical kinetics for single-molecule fluctuations of the OpdK protein channel (*4*), we have the following system of partial differential equations (*5-7*):

$$\frac{dP_{O1}}{dt} = -k_{O1\to O2}P_{O1} + k_{O2\to O1}P_{O2}$$
$$\frac{dP_{O2}}{dt} = +k_{O1\to O2}P_{O1} - k_{O2\to O1}P_{O2} + k_{O3\to O2}P_{O3} - k_{O2\to O3}P_{O2} \quad \text{(S1)}$$
$$\frac{dP_{O3}}{dt} = -k_{O3\to O2}P_{O3} + k_{O2\to O3}P_{O2}$$

where P_{O1}, P_{O2} and P_{O3} are the probabilities to occupy the O_1, O_2 and O_3 sub-states, respectively. These probabilities are defined by the following expressions (*5-7*):

$$P_{O1} = \frac{T_{O1}}{T} = \frac{N_{O1}\tau_{O1}}{T} = f_{O1}\tau_{O1}$$
$$P_{O2} = \frac{T_{O2}}{T} = \frac{N_{O2}\tau_{O2}}{T} = (f_{O1} + f_{O3})\tau_{O2} \quad \text{(S2)}$$
$$P_{O3} = \frac{T_{O3}}{T} = \frac{N_{O3}\tau_{O3}}{T} = f_{O3}\tau_{O3}$$

Here, T_{O1}, T_{O2} and T_{O3} are the total times occupied by the O_1, O_2 and O_3 sub-states, respectively. N_{O1}, N_{O2} and N_{O3} are the total recorded events that correspond to the O_1, O_2 and O_3 sub-states, respectively. T indicates the total recording time. f and τ denote the event frequency and the average dwell time for a well-defined sub-state, respectively. The equations (S2) show two components for the O_2 state, corresponding to transitions toward the O_1 and O_3 sub-states. In other words, the well made by the O_2 sub-state is flanked by two barriers for reaching the O_1 and O_3 sub-states.

The rates for reaching the O_1 and O_3 sub-states are just the corresponding event frequencies, which are normalized to the P_{O2} probability:

$$k_{O2\to O1} = \frac{f_{O1}}{P_{O2}} = \frac{f_{O1}}{1 - f_{O1}\tau_{O1} - f_{O3}\tau_{O3}}$$
$$k_{O2\to O3} = \frac{f_{O3}}{P_{O2}} = \frac{f_{O3}}{1 - f_{O1}\tau_{O1} - f_{O3}\tau_{O3}} \quad \text{(S3)}$$

At equilibrium, the partial derivatives of equations (S1) are zero, since the event probabilities are constant. Therefore,

$$k_{O1\to O2} = \frac{1}{\tau_{O1}}$$
$$k_{O3\to O2} = \frac{1}{\tau_{O3}} \quad \text{(S4)}$$

The equations (S3) and (S4) indicate that the four rates, which describe the kinetic scheme with three open sub-states, can be calculated using the event frequencies and the average dwell times of the flanked O_1 and O_3 sub-states. In addition, the equations (S3) and (S4) confirm the general rule that the average dwell time in a particular sub-state is given by the reciprocal of the sum of the kinetic rate constants for the transitions occurring away from that respective sub-state (*3;4;8;9*):

$$\frac{1}{\tau_{O2}} = k_{O2\to O1} + k_{O2\to O3} \quad \text{(S5)}$$

Table S3: The standard free energies corresponding to various gating transitions of the OpdK protein. (A) 1 M KCl; (B) 2 M KCl; (C) 3 M KCl; (D) 4 M KCl. The buffer solution contained 10 mM potassium phosphate, pH 8.0. All standard free energy (ΔG) values are given in k_BT. Data represent averages ± SDs over a number of at least three distinct single-channel electrical recordings.

A.

U (mV)	$\Delta G_{O1\rightarrow O2}$	$\Delta G_{O3\rightarrow O2}$
-80	-2.8 ± 0.2	-1.6 ± 0.1
-60	-3.4 ± 0.2	-1.6 ± 0.1
-40	-4.4 ± 0.5	-1.5 ± 0.1
-20	-4.9 ± 0.6	-1.8 ± 0.1
+20	-3.7 ± 0.1	-2.0 ± 0.1
+40	-3.4 ± 0.2	-1.6 ± 0.3
+60	-3.3 ± 0.5	-1.8 ± 0.2
+80	-2.6 ± 0.1	-1.6 ± 0.2

B.

U (mV)	$\Delta G_{O1\rightarrow O2}$	$\Delta G_{O3\rightarrow O2}$
-80	-3.0 ± 0.2	-1.2 ± 0.3
-60	-3.3 ± 0.4	-1.1 ± 0.3
-40	-3.6 ± 0.3	-0.8 ± 0.5
-20	-3.7 ± 0.1	-1.1 ± 0.4
+20	-3.5 ± 0.4	-1.1 ± 0.3
+40	-3.5 ± 0.4	-0.9 ± 0.3
+60	-3.3 ± 0.5	-1.4 ± 0.2
+80	-3.3 ± 0.5	-1.4 ± 0.2

C.

U (mV)	$\Delta G_{O1\rightarrow O2}$	$\Delta G_{O3\rightarrow O2}$
-80	-2.7 ± 0.3	-0.9 ± 0.5
-60	-3.3 ± 0.1	-0.9 ± 0.3
-40	-3.9 ± 0.2	-1.5 ± 0.1
-20	-4.0 ± 0.3	-1.3 ± 0.1
+20	-4.2 ± 0.3	-1.6 ± 0.3
+40	-4.0 ± 0.6	-1.4 ± 0.1
+60	-4.0 ± 0.9	-1.3 ± 0.1
+80	-3.6 ± 1.1	-1.1 ± 0.2

D.

U (mV)	$\Delta G_{O1\rightarrow O2}$	$\Delta G_{O3\rightarrow O2}$
-80	-3.2 ± 0.1	-0.4 ± 0.4
-60	-3.0 ± 0.1	-0.1 ± 0.4
-40	-3.6 ± 0.4	-0.2 ± 0.3
-20	-3.9 ± 0.2	-0.3 ± 0.2
+20	-4.8 ± 0.3	-0.4 ± 0.2
+40	-4.2 ± 0.6	-0.4 ± 0.3
+60	-4.1 ± 0.6	-0.4 ± 0.2
+80	-4.2 ± 0.6	-0.3 ± 0.2

Voltage dependence of the current amplitude of the discrete single-channel transitions. The current amplitudes of the $O_2 \rightarrow O_1$ and $O_2 \rightarrow O_3$ transitions are voltage dependent (**Fig. S1**). In the range -80 to +80 mV, both current amplitudes $I_{O2\text{-}O1}$ (the large-amplitude current blockades) and $I_{O3\text{-}O2}$ (the low-amplitude current transitions) are not linearly dependent on the applied transmembrane potential. On the other hand, at higher KCl concentrations, the slope of the $I_{O3\text{-}O2}$ current amplitude is greater than the corresponding value of the $I_{O2\text{-}O3}$ current amplitude.

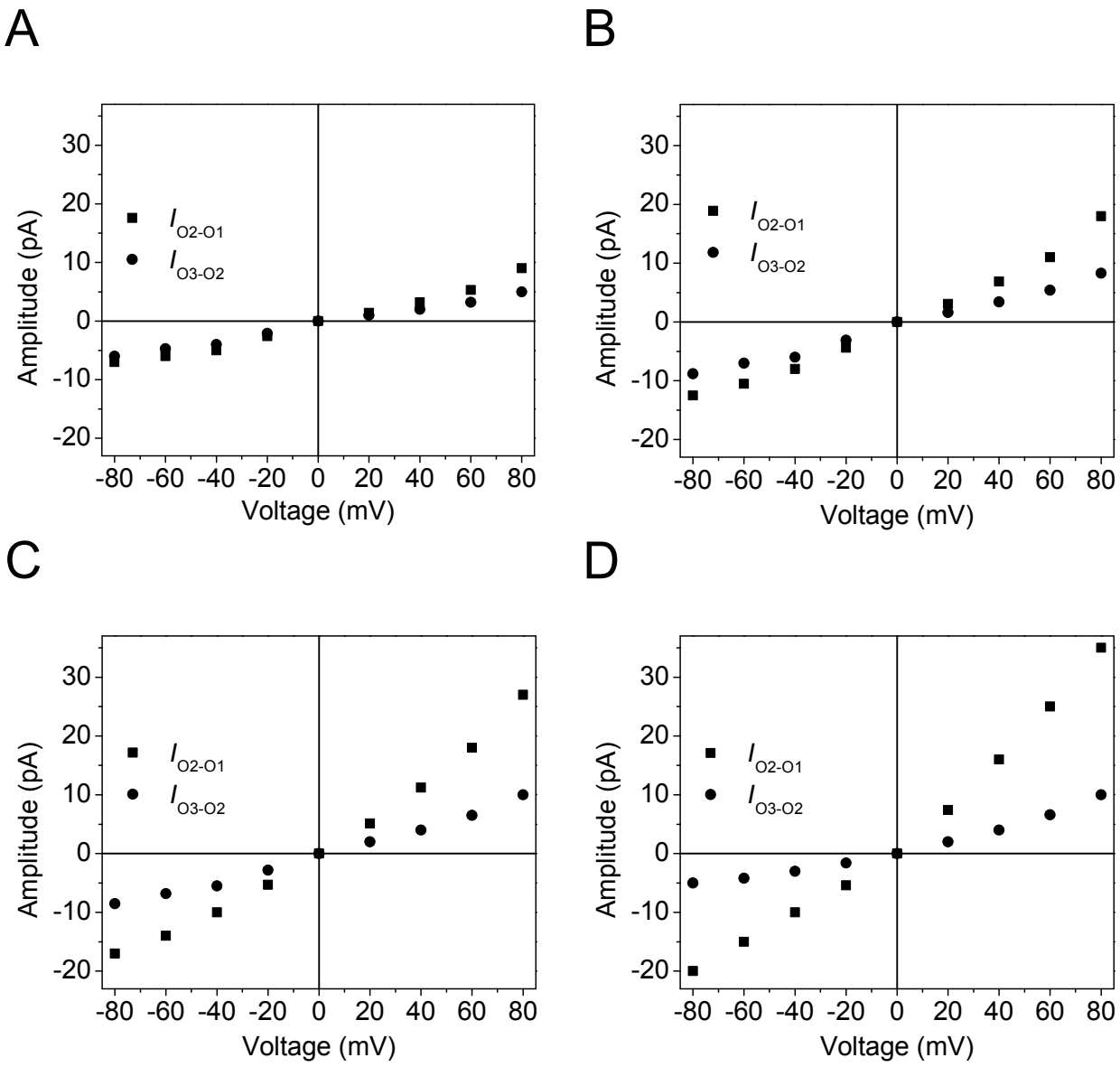

Figure S6: Voltage dependence of the current amplitudes of the single-channel transitions observed with the OpdK protein at various KCl concentrations. (A) 1 M KCl; (B) 2 M KCl; (C) 3 M KCl; (C) 4 M KCl. The buffer solution contained 10 mM potassium phosphate, pH 8.0.

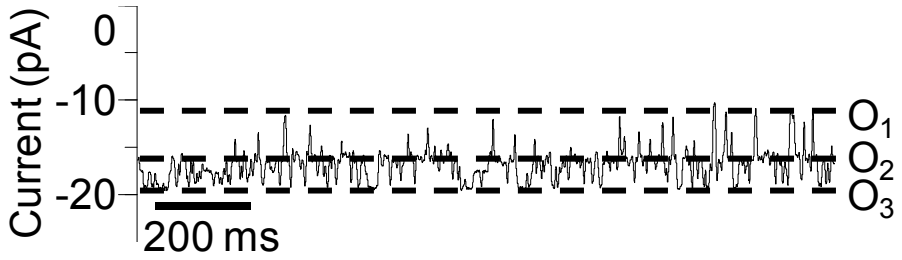

Figure S7: Single-channel electrical recordings with the OpdK protein in 500 mM KCl and at an applied transmembrane potential of -80 mV. The figure shows that the number of current sub-states is conserved. Under these conditions, the signal-to-noise ratio is low and the single-channel events are very short. This is the major reason for which we explored the single-channel channel kinetics of OpdK in greater KCl concentrations.

References

1. Biswas, S., Mohammad, M. M., Movileanu, L., and van den Berg, B. (2008) Crystal structure of the outer membrane protein OpdK from Pseudomonas aeruginosa, *Structure 16*, 1027-1035.

2. Jung, Y., Bayley, H., and Movileanu, L. (2006) Temperature-responsive protein pores, *J. Am. Chem. Soc. 128*, 15332-15340.

3. Mohammad, M. M. and Movileanu, L. (2008) Excursion of a single polypeptide into a protein pore: simple physics, but complicated biology, *Eur. Biophys. J. 37*, 913-925.

4. Aidley, D. J. and Stanfield, P. R. (1996) *Ion channels - Molecules in action* Cambridge University Press, Cambridge.

5. Urry, D. W., Venkatachalam, C. M., Spisni, A., Lauger, P., and Khaled, M. A. (1980) Rate theory calculation of gramicidin single-channel currents using NMR-derived rate constants, *Proc. Natl. Acad. Sci. U. S. A 77*, 2028-2032.

6. Kostyuk, P. G., Shuba, Y., and Teslenko, V. I. (1989) Activation kinetics of single high-threshold calcium channels in the membrane of sensory neurons from mouse embryos, *J. Membr. Biol. 110*, 29-38.

7. Moss, G. W. J. and Moczydlowski, E. (2002) Concepts of single-channel analysis: inferring function from fluctuations, in *Ion Channels - A Parctical Approach* (Ashley, R. H., Ed.) Second ed., pp 69-112, Oxford University Press, Oxford.

8. Goodrich, C. P., Kirmizialtin, S., Huyghues-Despointes, B. M., Zhu, A. P., Scholtz, J.M., Makarov, D. E., and Movileanu, L. (2007) Single-molecule electrophoresis of beta-hairpin peptides by electrical recordings and Langevin dynamics simulations, *J. Phys. Chem. B 111*, 3332-3335.

9. Bikwemu, R., Wolfe, A. J., Xing, X., and Movileanu, L. (2010) Facilitated translocation of polypeptides through a single nanopore, *J. Phys. :Condens. Matter 22*, 454117.